Dynamic behavior of 3a,4,4a,8-tetrahydro-4,4,8,8-tetramethyl-*tert*-butyl-4-stannaindacene

V. I. Mstislavsky, O. Yu. Savel´ev, and I. P. Gloriozov★

Department of Chemistry, M. V. Lomonosov Moscow State University, 1 Leninskie Gory, 119992 Moscow, Russian Federation. Fax: +7 (495) 939 2677. E-mail: gloriozov@nmr.chem.msu.su; savelyev@nmr.chem.msu.su

The stannotropic rearrangement in 3a,4,4a,8-tetrahydro-4,4,8,8-tetramethyl-*tert*-butyl-4-stanna-*symm*-indacene was studied by dynamic NMR spectroscopy. Line-shape analysis of the spectra with the use of various possible schemes of chemical exchange gives similar calculated spectra. The decision between three possible exchange schemes was made based on line-shape analysis, general structural considerations, and quantum chemical calculations. A comparison with the precursor, in which the Bu^t group is absent, shows that the presence of this group has an ambiguous effect on the activation barriers of rearrangements.

Key words: stannotropic rearrangement, activation parameters, dynamic NMR, line-shape analysis, quantum chemical calculations of energies of isomers.

Tetrahydro-*symm*-indacenes containing one or two Group IV metal atoms, *viz.*, η^1-cyclopentadienyl derivatives of these elements, are used as the starting reagents in the synthesis of catalytically active ansa-metallocenes.[1,2] Some of these compounds have been studied in depth. These compounds were found to consist of several isomers existing in equilibrium due to fast elementotropic rearrangements.[3,4]

3a,4,4a,8-Tetrahydro-4,4,8,8-tetramethyl-*tert*-butyl-4-stanna-*symm*-indacene (**A**), which has been synthesized earlier, also shows the dynamic behavior.[5] The NMR spectra recorded at different temperatures demonstrate that all four isomers of **A** are involved in mutual exchange.

Based on the known data on elementotropic rearrangements in cyclopentadiene derivatives of main-group elements,[6] the scheme of rearrangements involving isomers of compound **A** can be unambiguously constructed from its structure (Scheme 1). This scheme is rather complicated and is an object of investigation by complete line-shape analysis of dynamic NMR spectra. This was the main aim of the present study.

To investigate conversions of stannaindacene **A** by complete line-shape analysis of dynamic NMR and determine the activation parameters, we recorded the ^{119}Sn NMR spectra of this compound in the temperature range of 186—342 K. We chose toluene-d_8 as a solvent because it exists in the liquid state in this temperature range.

In the slow-exchange temperature region, the spectra show four lines with different intensities, each line corresponding to one particular isomer. Broadening of some lines in the spectra, which is associated with dynamic processes, was observed already at the lowest temperatures achieved in the experiments (186—210 K). At 330 K and higher temperatures, one averaged line is observed in the spectra.

Scheme 1

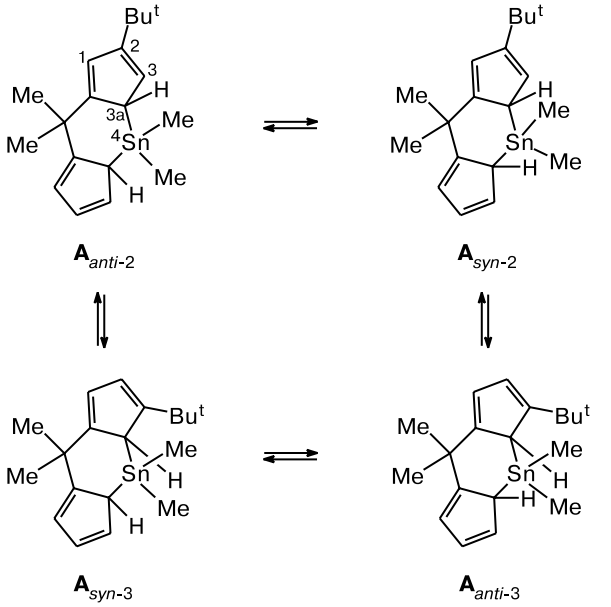

Isomers of **A** can be denoted according to their structures as $\mathbf{A}_{syn\text{-}2}$, $\mathbf{A}_{syn\text{-}3}$, $\mathbf{A}_{anti\text{-}2}$, and $\mathbf{A}_{anti\text{-}3}$, which reflect the *syn*- or *anti*-arrangement of the allylic protons in the cyclopentadienyl rings and the presence of the Bu^t group at position 2 or 3 of the cyclopentadienyl ring (see Scheme 1).

Published in Russian in *Izvestiya Akademii Nauk. Seriya Khimicheskaya,* No. 10, pp. 2286—2290, October, 2005.

1066-5285/05/5410-2359

The assignment of the signals in the ^{119}Sn NMR spectra to particular isomers of **A** is of fundamental importance. Simulation programs for dynamic NMR line-shape analysis simulate exchange processes between the positions of nuclei corresponding to the observed spectral lines. It may be that these model processes do not occur in real situation. The correct assignment is necessary for the calculated processes to correspond to real processes that occur, in the case under consideration, between isomers $\mathbf{A}_{syn\text{-}2}$, $\mathbf{A}_{syn\text{-}3}$, $\mathbf{A}_{anti\text{-}2}$, and $\mathbf{A}_{anti\text{-}3}$.

According to Scheme 1, four interconversions occur in the system, each isomer of **A** being involved in two of these processes. There are three possible alternative schemes of conversions between four different objects (in this case between the isomers), which are enumerated in order of increasing energies (Scheme 2, *A*—*C*).

Scheme 2

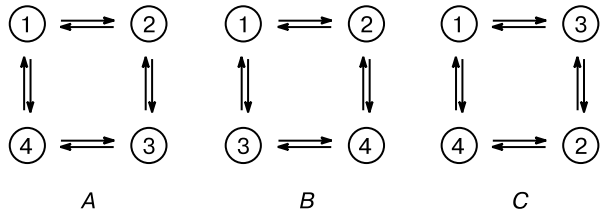

Complete line-shape analysis with the use of an adequate scheme for the description of the spectral problem can give the correct activation parameters of processes, even if it is unknown (due to the lack of precise assignment), which isomeric structures are involved in these processes. There are 24 possible assignments of four lines to four objects, each assignment corresponding to one of alternatives presented in Scheme 2 (*A*, *B*, or *C*).

In the case under consideration, the simplest and most reliable procedure for the assignment of lines is based on the relationship between the integrated intensity of the latter and the thermodynamic energies of the equilibria between isomers.

Evident limitations (based on the steric factor of the arrangement of the Bu^t group)

$$E_{syn\text{-}3} > E_{syn\text{-}2},\ E_{anti\text{-}3} > E_{anti\text{-}2}$$

reduce the number of possible assignments to six. However, none of alternatives presented in Scheme 2 can be ruled out in this case. If the following additional limitations (which, together with the above-mentioned limitations, are based on the hypothesis that the position of the Bu^t group is the determining factor for the energy of this structure) are taken into account

$$E_{syn\text{-}3} > E_{anti\text{-}2},\ E_{anti\text{-}3} > E_{syn\text{-}2},$$

we have four possible assignments corresponding to Schemes 2, *A* and 2, *B*.

To make the unambiguous assignment of the lines, we performed quantum-chemical calculations of the energies of structures $\mathbf{A}_{syn\text{-}2}$, $\mathbf{A}_{syn\text{-}3}$, $\mathbf{A}_{anti\text{-}2}$, and $\mathbf{A}_{anti\text{-}3}$. We used the density functional method with the nonlocal functional PBE constructed nonempirically[7] and the TZ2p basis set implemented in the PRIRODA program package.[8,9] Earlier, we have successfully used this program package for solving analogous problems.[10,11] Since relativistic corrections are of considerable importance in calculations of structures and reactivities of compounds containing atoms of the fourth and higher periods, we used the SBK effective core potential.[12] The molecular geometry (Fig. 1) was optimized using the total energy criterion. The zero-point energies E_{ZPV} were calculated for the optimized geometry. The zero-point energy corrections were determined in the harmonic approximation.

The calculated energies are given in Table 1. The total energies of the molecules (E) and the energies with zero-point energy correction $E_0 = E + E_{ZPV}$ are given in Hartree atomic units, and the enthalpies ($\Delta H°$), which are equal to $\Delta G°$ at 0 K, are given in kJ mol^{-1} (taking into account that 1 a.u. = 2625.50 kJ mol^{-1}).

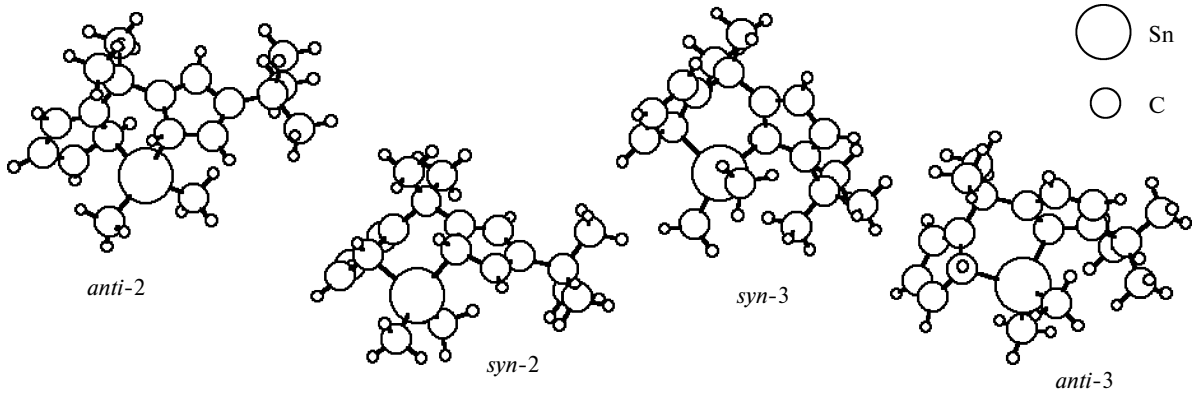

Fig. 1. Structures of isomers of stannaindacene **A** calculated by the quantum-chemical method with geometry optimization.

Table 1. Energies of isomers of stannaindacene **A** (total energies (E) and energies with zero-point energy correction (E_0)) calculated by the quantum-chemical method

Isomer **A**	$-E$	$-E_0$	$E_0 - E_0(\mathbf{A}_{anti\text{-}2})$	$\Delta(\Delta H^\circ)$ /J mol^{-1}
	a.u.			
anti-2	127.948260	127.547366	0.00	0.0
syn-2	127.948136	127.546950	0.000416	1092.21
syn-3	127.944719	127.543416	0.003950	10370.7
anti-3	127.944376	127.543073	0.004293	11271.3

Therefore, according to the results of quantum-chemical calculations at 0 K, the isomers are arranged in order of increasing energies E and E_0 as follows:

$\mathbf{A}_{anti\text{-}2}$, $\mathbf{A}_{syn\text{-}2}$, $\mathbf{A}_{syn\text{-}3}$, $\mathbf{A}_{anti\text{-}3}$.

An increase in the temperature leads to an increase in the energy of molecules due to an increase in the population of the excited vibrational levels. However, the energies of isomers are, as a rule, increased proportionally, and the zero-point vibrations make the main contribution. Hence, let us assume that the arrangement of isomers in order of increasing energies remains unchanged in the temperature range of 0—186 K, and, consequently, the correct assignment of the lines corresponds to Scheme 2, *B* (Table 2).

The above-described arrangement of isomers in order of increasing energies differs from that proposed earlier.[5] The latter assignment was tentative, because this question has not been considered in detail.[5]

The Gibbs energies of the equilibria between isomers at 186 K, which were calculated from the integrated intensities, are also given in Table 2. The confidence interval was estimated assuming that the accuracy of single direct measurements of the integrals is 10%. In this case, the intervals are similar in size.

It should be noted that the energy differences $\Delta H^\circ = \Delta G^\circ$ (0 K) between isomers with different arrangement of the Bu^t group, which were determined from quantum-chemical calculations, are substantially larger than the energy differences (ΔG° at 186 K) estimated from the experimental intensities. Apparently, this discrepancy is also not associated with the temperature factor. Presumably, this is the manifestation of the influence of the solvent on the energy of molecules in solution. The calculations were carried our for isolated molecules, whereas molecules of a dissolved compound interact with the solvent in solution.

Table 2. Assignment of the lines in the ^{119}Sn NMR spectrum of stannaindacene **A** at 186 K and the Gibbs energies of the equilibria between isomers (ΔG°) at 186 K

Number*	Isomer **A**	δ/Hz	I**	ΔG° /J mol^{-1}
1	*anti*-2	44915.0	36.049	0.0
2	*syn*-2	42859.0	11.052	1828.3±218
3	*syn*-3	46781.0	6.428	2665.5±218
4	*anti*-3	42150.9	1.00	5543.9±219

* The number corresponds to the number of the isomer shown in Scheme 2 (in order of increasing energies).
** The integrated intensity.

Dynamic NMR line-shape analysis was carried out independently for all alternatives presented in Scheme 2. To obtain the best agreement between the experimental and calculated spectra, we optimized the following temperature-independent parameters:[13—15] 1) the sought activation parameters of the processes, $\Delta G^{\neq}_{\alpha}(T_0)$, $\Delta S^{\neq}_{\alpha}$ (T_0 is the fixed temperature (298 K) and α (1—4) is the number of the process); 2) the entropy parameters of the equilibrium ΔS°_μ (μ = 2—4, the number of the isomer); 3) the intrinsic linewidths ^0w_i (i is the number of the line); 4) the parameters of the temperature dependence of the resonance frequencies $^1\nu_i$ and $^2\nu_i$.

The activation parameters of the processes were optimized by line-shape analysis of the total set of spectra. The entropy parameters of the equilibrium and the intrinsic linewidths were optimized using the spectra in the slow-exchange temperature region. The parameters of the temperature dependence of the resonance frequencies were optimized based on the slow- and fast-exchange regions of the spectra.

In the optimization of the parameters with the use of the computer program, the following sum

$$S = \sum_{n}^{N_{pt}} (I_n^{exp} - I_n^{calc})^2$$

was minimized, where N_{pt} is the number of points in all spectra, n is the number of the point, and I is the intensity. The R factor is a more clear numerical criterion

$$R = \sqrt{S/S_0},$$

where

$$S_0 = \sum_{n}^{N_{pt}} (I_n^{exp})^2.$$

In addition to the numerical criterion, we estimated the visual correspondence of the spectra. The latter is often more reliable when fine features of the spectra are compared.

As a result, we failed to achieve a satisfactory agreement for Scheme 2, *C*. For Schemes 2, *A* and 2, *B*, we obtained a good agreement between the experimental and calculated lines. The *R* factor is 0.147 and 0.141 for schemes 2, *B* and 2, *A*, respectively (spectra were normalized to the integral equality in the whole temperature range). This difference cannot be considered as quite significant to decided between these exchange schemes taking into account that the visual correspondence is also equally good.

The activation parameters ($\Delta G^{\neq}$, $\Delta S^{\neq}$) and the values of $\Delta H^{\neq}$ ($\Delta H^{\neq} = \Delta G^{\neq} + T_0\Delta S^{\neq}$) calculated from these parameters are given in Table 3.

Since the agreement between the calculated and experimental lines achieved with the use of two different schemes is almost the same, additional studies were required to solve this problem. We performed simulations of the experiment to estimate the distance between the sets of lines calculated according to two schemes for all possible parameter sets. For this purpose, we optimized the parameters in one exchange scheme to fit the line shape to the spectra calculated according to another scheme in the absence of noise. Finally, we failed to overcome a certain visual discrepancy, but we obtained small numerical values of the *R* factor: 0.103 by approximating Scheme 2, *B* to the spectra obtained from Scheme 2, *A*, and 0.093 by approximating Scheme 2, *A* to 2, *B* (normalization to the integral equality).

Therefore, we found that this spectral problem is ambiguous. Thus, different exchange schemes can approximate a certain line shape (experimental), which are only slightly different in the degree of correspondence. In other words, different combinations of mutual exchanges between four isomers give very similar spectral line shapes. Presumably, this is associated with the cyclic character of the processes.

In this case, the line shape is little informative for the choice of the exchange scheme. In this case, line-shape analysis allows one to determine the activation parameters if the scheme is known in one way or another.

Apparently, the agreement was not achieved for Scheme 2 *C* due to the fact that the exchange between isomers 1 and 2, which is not involved in this scheme, is the determining factor for the line shape.

Therefore, complete dynamic NMR line-shape analysis enables one to estimate the validity of alternative schemes of the processes. However, in the case under consideration, this method provides only partial estimates. Hence, it is necessary to employ additional methods. The method used for quantum-chemical calculations of the energies of molecules led us to conclude that Scheme 2, *B* is true (see Table 3).

A comparative presentation of the experimental spectra and the spectra calculated according to Scheme 2, *B* is shown in Fig. 2.

The activation parameters of the isomeric conversion in the precursor of **A**, *viz.*, 3a,4,4a,8-tetrahydro-4,4,8,8-tetramethyl-4-stannaindacene (**B**), in which the Bu^t group is absent, have been determined earlier.[4] The latter compound exists as two isomers with the *syn* and *anti* arrangement of the allylic protons and the concentration ratio of 2 : 1 at 183 K, and these isomers undergo an interconversion. For the rearrangement of $\mathbf{B}_{syn}$ and $\mathbf{B}_{anti}$, the following activation parameters were estimated by complete line-shape analysis of dynamic NMR: $\Delta G^{\neq}_{298}$ = 49380±250 J mol^{-1}, $\Delta S^{\neq} = -21.5\pm4.0$ J mol^{-1} K^{-1}, and $\Delta H^{\neq} = 42980\pm860$ J mol^{-1}.

A comparison of these values with the results obtained for compound **A** shows that the introduction of the Bu^t group into the cyclopentadienyl ring has a complex effect on the activation barriers, an increase in the height of particular barriers being caused by a strong decrease in the activation entropy.

Table 3. Activation parameters of rearrangements of stannaindacene **A** determined from dynamic NMR line-shape analysis

Process	$\Delta G^{\neq}_{298}$ /J mol^{-1}	$\Delta S^{\neq}$ /J mol^{-1} K^{-1}	$\Delta H^{\neq}$ /J mol^{-1}
	Scheme 2, *B*		
1 ⇄ 2 ($\mathbf{A}_{anti\text{-}2}$ ⇄ $\mathbf{A}_{syn\text{-}2}$)	50014.7±30.7	−51.4±0.7	34692.7
1 ⇄ 3 ($\mathbf{A}_{anti\text{-}2}$ ⇄ $\mathbf{A}_{syn\text{-}3}$)	67255.5±320.0	−12.2±8.0	63623.1
2 ⇄ 4 ($\mathbf{A}_{syn\text{-}2}$ ⇄ $\mathbf{A}_{anti\text{-}3}$)	48862.0±6198.0	0.0±89.4	48862.0
3 ⇄ 4 ($\mathbf{A}_{syn\text{-}3}$ ⇄ $\mathbf{A}_{anti\text{-}3}$)	60705.3±109.5	−150.5±2.3	15860.7
	Scheme 2, *A*		
1 ⇄ 2	48916.2±40.0	−36.6±0.9	38021.2
1 ⇄ 4	55178.7±582.8	−36.4±22.6	44343.8
2 ⇄ 3	69093.7±593.9	−83.8±20.8	44137.3
3 ⇄ 4	60874.74±113.1	−156.8±2.6	14157.2

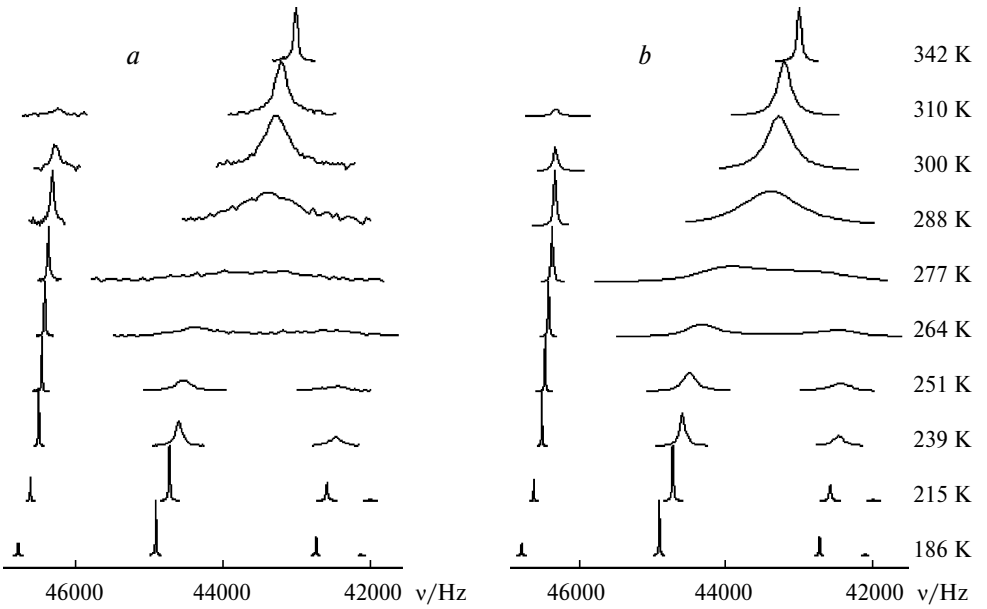

Fig. 2. Experimental ^{119}Sn NMR spectra of stannaindacene **A** (*a*) and spectra calculated according to Scheme 2, *B* (*b*).

Experimental

The ^{119}Sn NMR spectra were recorded on a Varian VXR-400 spectrometer. The temperature detector of the spectrometer was calibrated against methanol at low temperatures and against ethylene glycol at high temperatures. Toluene-d_8 was used as solvent. The tube with the sample was sealed. The standard (Me_4Sn) was not added, because it gives a signal in the region of the observed signals. Hence, we determined the chemical shifts (see Table 2) relative to the arbitrary zero point, which is quite sufficient for solving the problem under consideration, because line-shape analysis requires a knowledge of only the difference in the chemical shifts of the isomers involved in the exchange.

Quantum-chemical calculations were carried on an MBC 1000M computer cluster in the Joint Supercomputer Center of the Russian Academy of Sciences (Moscow).

The dynamic NMR line-shape analysis was carried out on a PC using the DISPARD program.[13]

References

1. I. E. Nifant´ev, M. V. Borzov, A. V. Churakov, S. G. Mkoyan, and L. O. Atovmyan, *Organometallics*, 1992, **11**, 3942.
2. M. Hüttenhofer, M.-H. Prosenc, R. Rief, F. Schaper, and H.-H. Brintzinger, *Organometallics*, 1996, **15**, 4816.
3. I. E. Nifant´ev, A. K. Shestakova, D. A. Lemenovskii, Yu. L. Slovokhotov, and Yu. T. Struchkov, *Metalloorg. Khim.,* 1991, **4**, 292 [*Organomet. Chem. USSR*, 1991, **4** (Engl. Transl.)].
4. I. E. Nifant´ev, V. L. Yarnykh, M. V. Borzov, B. A. Mazurchik, V. I. Mstislavsky, V. A. Roznyatovsky, and Y. A. Ustynyuk, *Organometallics*, 1991, **10**, 3739.
5. I. E. Nifant´ev, M. V. Borzov, P. V. Ivchenko, V. L. Yarnykh, and Y. A. Ustynyuk, *Organometallics*, 1992, **11**, 3462.
6. P. Jutzi, *Chem. Rev.*, 1986, **86**, 983.
7. J. P. Perdew, K. Burke, and M. Ernzerhof, *Phys. Rev. Lett.*, 1996, **77**, 3865.
8. D. N. Laikov, *Chem. Phys. Lett.*, 1997, **281**, 151.
9. D. N. Laikov and Yu. A. Ustynuk, *Izv. Akad. Nauk, Ser. Khim.*, 2005, 804 [*Russ. Chem. Bull., Int. Ed.*, 2005, **54**, 820 (Engl. Transl.)].
10. Yu. A. Ustynuk, L. Yu. Ustynuk, D. N. Laikov, and V. V. Lunin, *J. Organomet. Chem.*, 2000, **579**, 182.
11. E. D. Smurnyi, I. P. Gloriozov, and Yu. A. Ustynyuk, *Zh. Fiz. Khim.*, 2003, **77**, 1888 [*Russ. J. Phys. Chem.*, 2003, **77**, 1699 (Engl. Transl.)].
12. W. J. Stivens, H. Basch, V. Krauss, and P. Jasien, *Can. J. Chem.*, 1992, **70**, 612.
13. V. I. Mstislavsky, Ph. D. (Phys.-Mat.) Thesis, M. V. Lomonosov Moscow State University, Moscow, 1985, 190 pp. (in Russian).
14. R. Laatikainen, *J. Magn. Reson.*, 1985, **64**, 375.
15. V. I. Mstislavsky and N. M. Sergeyev, *14 Discussiontagung der Fachbereich "Magnetische Resonanzspectroscopie,"* Witzenhausen (BRD), September 1992, 37.

Received April 8, 2005;
in revised form July 28, 2005